AD-756 897

SPATIAL COHERENCE OF SURFACE WAVES

H. Mack

Teledyne Geotech

8

.......contributing to man's
understanding of the environment world

SPATIAL COHERENCE
OF SURFACE WAVES

H. MACK

SEISMIC ARRAY ANALYSIS CENTER

20 DECEMBER 1972

D D C
RECEIVED
JAN 17 1973
B

▼TELEDYNE GEOTECH
ALEXANDRIA LABORATORIES

DOCUMENT CONTROL DATA - R&D

(Security classification of title, body of abstract and indexing annotation must be entered when the overall report is classified)

1 ORIGINATING ACTIVITY *(Corporate author)*	2a. REPORT SECURITY CLASSIFICATION
Teledyne Geotech	Unclassified
Alexandria, Virginia 22314	2b. GROUP

3 REPORT TITLE

SPATIAL COHERENCE OF SURFACE WAVES

4 DESCRIPTIVE NOTES *(Type of report and inclusive dates)*

Scientific

5 AUTHOR(S) *(Last name, first name, initial)*

Mack, H.

6 REPORT DATE	7a. TOTAL NO. OF PAGES	7b. NO. OF REFS
20 December 1972	~~40~~ 41	11

8a. CONTRACT OR GRANT NO.	9a. ORIGINATOR'S REPORT NUMBER(S)
F33657-72-C-0471	
b. PROJECT NO	8
VELA T/2709	
ARPA Order No. 1620	9b. OTHER REPORT NO(S) *(Any other numbers that may be assigned this report)*
Program Code 2F10	

10 AVAILABILITY/LIMITATION NOTICES

APPROVED FOR PUBLIC RELEASE; DISTRIBUTION UNLIMITED.

11 SUPPLEMENTARY NOTES	12. SPONSORING MILITARY ACTIVITY
	Advanced Research Projects Agency
	Nuclear Monitoring Research Office
	Arlington, Virginia 22209

13 ABSTRACT

Using spatial coherency estimates of Rayleigh and Love waves recorded at ALPA, LASA and NORSAR, it is demonstrated that for a particular frequency the wave propagation cannot be described by a unique wavevector. Instead, the propagation is better described by a distribution in the wavenumber domain or, in physical terms, a distribution in azimuth and phase velocity. In general the coherency in the mean direction of propagation, which is a function of the velocity distribution, stays high relative to the coherency along the mean wavefront, which is a function of the azimuthal distribution.

14 KEY WORDS

Spatial Coherence
Surface Waves
Large Arrays

SPATIAL COHERENCE OF SURFACE WAVES

SEISMIC ARRAY ANALYSIS CENTER REPORT NO. 8

AFTAC Project Number: VELA T/2709

Project Title: Seismic Array Analysis Center

ARPA Order No.:   1620

ARPA Program Code No.:   2F10

Name of Contractor: Teledyne Geotech

Contract No.:   F33657-72-C-0471

Effective Date of Contract: 1 January 1972

Amount of Contract: $1,663,848

Contract Expiration Date: 30 June 1973

Project Manager: Harry Mack
                           (703) 836-3882

P. O. Box 334, Alexandria, Virginia

TABLE OF CONTENTS

ic

LIST OF FIGURES

LIST OF FIGURES (Cont'd.)

INTRODUCTION

Large arrays of seismometers allow us to study how seismic signals vary over an area of the earth's surface. Some idea of the nature of this variation, and its magnitude, is necessary for array design and subsequent data processing. One measure of this variation is the coherence of the time shifted waveform between seismometer pairs. This paper presents experimental results for the variation of long period surface waves at the three large arrays ALPA, LASA and NORSAR.

Previous seismic coherence studies have been confined to long-period noise (Capon, 1969), short-period isotropic noise (Aki, 1957, and Backus, et al, 1964), and short-period directional noise (Bungum, et al, 1971). However, the earth is not homogeneous and so the waveform of a 'pure' signal changes as it propagates, due to refraction, diffraction, dispersion, and scattering. This change of waveform causes a loss of coherence which depends on the seismometer separation and the wave frequency. There is a further coherence loss due to the additive background noise but in this study only signals with large signal-to-noise ratios are used and so the coherence loss caused by the background is considered to be negligible.

SPATIAL COHERENCE AND PROPAGATION

When a surface wave propagates in a medium which has lateral inhomogeneities comparable in scale to the wavelength, the constant phase surfaces of the wave are neither simply planar nor cylindrical. The wave fronts cannot be represented by a single wave vector at each frequency. For a time window of particular length used in analysis, the wave vector at each frequency has a distribution both in magnitude and direction, or, in other words, a particular frequency component of the wave does not have a unique phase velocity or arrival azimuth. The wave is then represented in wavenumber space as a distribution $F(\underline{k})$ rather than a singularity $\delta(\underline{k}-\underline{k}_0)$ at a particular frequency. The spatial coherence $\gamma(f,\underline{r})$ is then defined as:

$$\gamma(f,\underline{r}) = \frac{1}{N}\left|\int_K F(\underline{k},f)\exp(-2\pi i\underline{k}\cdot\underline{r})dk\right| \tag{1}$$

The integration is taken over the area K, which is the region in the wavenumber domain where $F(\underline{k}) \neq 0$. N is a suitable normalizing factor.

Consider a signal recorded at two sites separated by a distance r. The coherence between the two at a frequency f is normally defined as:

$$\gamma^2_{12}(f) = \frac{\left|G_{12}(f)\right|^2}{G_1(f)G_2(f)} \tag{2}$$

-2-

where

$G_{12}(f)$ = cross power spectrum at frequency f

$G_1(f)$ = power spectrum at site 1

$G_2(f)$ = power spectrum at site 2

By estimating the coherence of the signals between all seismometer pairs in an array, the spatial variation of the coherence $\gamma(f,\underline{r})$ can be obtained, where $\underline{r}$ is the vector separation of any two positions within the array. The wavenumber distribution $F(\underline{k})$ responsible for the spatial coherence can then be obtained by inversion of expression (1). If the distribution $F(\underline{k})$ is confined to a relatively small region of wavenumber space, it has been demonstrated theoretically (Gossard, 1969) and experimentally (Mack and Flinn, 1971) that the two-dimensional transformation of expression (1) can be well approximated by independent one-dimensional transformations, with the result that the variation in coherence in the direction of propagation is a function of the wavenumber magnitude range (and hence the velocity range) whereas the variation in coherence normal to the direction of propagation is only a function of the angular distribution of $F(\underline{k})$. To illustrate this consider the wavenumber geometry shown in Figure 1.

The wavefield is represented by an area of finite thickness $2\Delta k$ subtending an angle $\pm \theta$ about the origin. This wavenumber geometry describes a wave group propagating, on the average, in the negative Y direction. The

words "on the average" are used because the azimuth of propagation is really distributed ± 0 about the Y axis. Similarly the magnitude of the wavevector is distributed as $k_o \pm \Delta k$. Physically, this means that the phase velocity has a distribution rather than a unique value at a particular frequency, within the area of the array. The range of velocity is given by:

$$(v_1, v_2) = (\frac{f}{k_o - \Delta k}, \frac{f}{k_o + \Delta k}) \tag{3}$$

If only small spread angles and velocity ranges are considered, as was mentioned before, the coherence loss in the wavefront direction is virtually independent of the loss in the wave propagation direction. This is equivalent to making the region K rectangular, in which case the integral (1) becomes the product of two simple integrals.

$$\gamma(\underline{r}, f) = \frac{1}{2k_o \sin\theta} \int_{-k_o \sin\theta}^{k_o \sin\theta} F(k_x, f) \exp(-2 ik_x x \, dkx$$

$$\tag{4}$$

$$\cdot \frac{1}{2\Delta k} \int_{k_o - \Delta k}^{k_o + \Delta k} F(k_y, f) \exp(-2\pi ik_y y) dk_y$$

For various simple forms of $F(\underline{k})$, equation (4) can easily be solved. The four forms

1. $F(k_x) = 1$, $F(k_y) = 1$

2. $F(k_x) = \exp(-\alpha|k_x|)$, $F(k_y) = \exp(-\beta|k_y - k_o|)$

3. $F(k_x) = \exp(-\alpha k_x^2)$, $F(k_y) = \exp(-\beta(k_y-k_o)^2)$

4. $F(\underline{k}) = \delta(\underline{k}-\underline{k}_1) + \delta(\underline{k}-\underline{k}_2)$

imply spatial coherence of the forms:

1. $\gamma(\underline{r},f) = \dfrac{\sin(2\pi k_o x \sin\theta)}{2\pi k_o x \sin\theta} \cdot \dfrac{\sin(2\pi\Delta k y)}{2\pi\Delta k y}$

2. $\gamma(\underline{r},f) = \dfrac{2\alpha}{\alpha^2 + 4\pi x^2} \cdot \dfrac{2\beta}{\beta^2 + 4\pi y^2}$

3. $\gamma(\underline{r},f) = \left(\dfrac{\pi}{\alpha}\right)^{\frac{1}{2}} \exp\left(-\dfrac{\pi^2 x^2}{\alpha}\right) \cdot \left(\dfrac{\pi}{\beta}\right)^{\frac{1}{2}} \exp\left(-\dfrac{\pi^2 y^2}{\beta}\right)$

4. $\gamma(\underline{r},f) = [1 + \cos 2\pi(\underline{k}_2-\underline{k}_1)\cdot\underline{r}]/2$

These expressions have the property that for y=0 the coherence parallel to the wavefront is a function of the angular scatter, and similarly for x=0 the coherence normal to the wavefront is a function of the velocity scatter.

Model (1) is perhaps physically unreasonable in the sense that it is difficult to imagine a scattering process where the scattered waves have the same amplitude within a certain angle and zero everywhere else. Some

sort of decay with increasing angle is more to be expected. Models (2) and (3) satisfy this condition. However, there is not much difference numerically in the three models for given ranges of scattering and all three have similar shapes, i.e., an increasingly negative first derivative in the region of small separation.

Models (2) and (3) are suggested by Chernov (1960) for wave propagation in random media. Model (4) is the expression which is representative of the multipathing phenomenon described by Capon (1969). Two or more discrete waves associated with the same phase (e.g., a Rayleigh wave) propagate across the array and so exhibit two distinct wavevectors. This last form causes the most severe variations in spatial coherence.

Figures 2 and 3 show theoretical curves for coherence (γ^2) versus seismometer separation for the case of Model (1) at a period of 21.3 seconds. In Figure 2 the separation is taken along the mean wavefront and the various curves illustrate how the coherence varies with increasing angular scatter. Figure 3 shows coherence versus separation in the direction of propagation for various velocity ranges. Figure 4 and 5 show the spatial coherence behavior at a period of 25.6 sec, again for Model (1). These particular periods are used in the theoretical examples because with the window length used in the spectral analysis these two discrete frequencies lay in the part of the spectrum having the most power. Figure 6 illustrates the effect of multipathing, using Model (4), on spatial coherence. Using such standard curves for comparison with coherence measured in the

-6-

two orthogonal directions allows the principal dimensions of the wavenumber distribution to be estimated and hence the angular scatter and velocity scatter of the wave.

Effect of dispersion

In estimating the coherency of a wave train between two points it might be assumed that dispersion would contribute to the loss of coherence in the direction of propagation. The phase relationship within a band of frequencies would vary with time, hence propagation distance.

This would cause changes in the real and imaginary parts of the Fourier transform which are smoothed separately in the coherence estimation. Using the phase velocity dispersion curve for LASA given by Glover and Alexander (1969), a synthetic example was used to determine the dispersion contribution to the coherency loss. The result was that for a distance separation of 100 km the coherence was still as high as 0.99 for a period of 20 seconds. It will be seen that the observed coherence loss is significantly greater than this so it is reasonable to assume that dispersion contributes very little to the form of the observed spatial coherency at LASA. It has been assumed that the result would be similar at NORSAR and ALPA.

COHERENCE ESTIMATES OF RAYLEIGH WAVES

Estimates have been made of the spatial variation of the coherence of surface waves at LASA, NORSAR and ALPA. The signals were aligned before the transformations and subsequent spectral smoothing were performed. Alignment is necessary in order to eliminate the phase shift caused by the relative delays across the array. Smoothing a spectrum which includes such a phase shift leads to an erroneous value for the cross power spectrum and hence an incorrect coherency estimate. Twenty-four degrees of freedom were used in the coherency estimation resulting in acceptably narrow confidence intervals at the 90% level.

NORSAR

Two examples using NORSAR recordings are presented to illustrate the azimuthal dependence of spatial coherence. Figure 7 shows the spatial coherence of a Rayleigh wave from an earthquake in North Sinkiang, the individual channels being shown in Figure 8. The period under consideration is 21.3 seconds; and, although there appears to be a small separation in the two orthogonal directions, the overall coherence remains high across the maximum extremities of the array. Comparison of the measured results with standard curves reveals that an angular scatter of ± 4° about the mean azimuth explains the loss of coherence along the wavefront. The slight decrease of coherence in the direction of propagation can be explained in terms of a phase velocity scatter

of approximately ± 0.1 km/sec about the mean value.

The spatial coherence of the Love wave at the same period is shown in Figure 9. Again the coherence remains high across the array and has about the same distribution as the Rayleigh wave.

At other azimuths the picture can be decidedly different. Figures 10 and 11 show a Turkish event recorded at NORSAR and the spatial coherence of the Rayleigh wave respectively. The signal-to-noise ratio is high and the signal appears visually to have little variation across the array. However, the spatial coherence falls off much more rapidly with sensor separation than in the previous case. The difference in coherence in the two orthogonal directions is now very obvious. In this situation lines of equal coherence are roughly elliptical with the major axis pointing in the mean direction of propagation. If the angular distribution is continuous, as in Models (1-3), a scatter of ± 10° about the mean direction explains the loss of coherence along the wavefront. If the variation is attributable to two discrete, equal-amplitude, interfering waves, represented by Model (4), then the azimuthal separation is about 12°.

The loss of coherence in the direction of propagation is somewhat scattered but a standard curve for a velocity range of ± 0.3 km/sec about a mean value lies through the measured values. If this coherency loss is caused by two discrete waves, or modes, propagating from the same back azimuth the phase velocity difference is approximately 0.25 km/sec.

ALPA

The Sinkiang event used in the NORSAR analysis was also analyzed using the ALPA recordings. The individual channels and beam are shown in Figure 12 and the spatial coherence of the Rayleigh wave at a period of 21.3 sec is shown in Figure 13. It is obvious that the loss of coherence along the mean wavefront is quite severe and corresponds to a continuous angular distribution of ± 20° or to two discrete waves separated by 30°.

Frequency wavenumber analysis of this particular Rayleigh wave showed the primary arrival crossing the array with a back azimuth of 314°. A second Rayleigh wave, presumably multipathed, crossed the array with a back azimuth of about 350° almost at the same time. This would certainly explain the rapid decrease in coherence.

The scatter in the coherence, even though the signal-to-noise ratio is very high, suggests that the scattering is more complex than can be explained by just one of the models.

Presumably a 'discrete' multipathed arrival has a finite distribution in the wavenumber plane so the measured spatial coherence would be affected by both.

The loss of coherence in the direction of propagation is rather scattered but appears to decrease in a consistent manner with increased separation. A curve passing through the points indicates that a velocity scatter of about ± 0.35 km/sec about a mean value could explain this. However this value may be too high

because the assumption that the coherence is independent in the two orthogonal directions starts to be invalid for wavenumber distributions which subtend angles greater than 20° (Gossard and Sailors, 1970).

In an attempt to estimate how much scattering occurs in the Alaskan region itself, the Rayleigh waves generated by Cannikin on Amchitka Island and recorded at ALPA were subjected to the coherency analysis. The results are shown in Figure 14. The separation in the two orthogonal directions is again quite striking. Even though the epicentral distance is only about 20° the loss of coherence along the wavefront suggests scattering over a range ± 12° about the mean azimuth. The coherence remains very high in the direction of propagation which indicates that the phase velocity at this period is almost single valued or, in other words, there is very little velocity scatter or mode mixing.

The lower spatial coherency values at ALPA with respect to NORSAR for Central Asian events helps to explain the constant surface wave magnitude difference for the same event measured at both arrays (Mack, 1972). The marked difference in coherence in the two directions suggests that elliptical arrays with the major axis pointing towards the source would give the best signal-to-noise ratio improvement. This has been demonstrated for some Rayleigh waves recorded at ALPA.

LASA

The two events used to investigate spatial coherence at the LASA also highlight the difference between the

scattering of a 'pure' Rayleigh wave and a multipathed example. Figure 15 illustrates the latter situation. In Figure 15a the orthogonal estimates of coherence are shown for a window 400 seconds long and in Figure 15b this has been extended to 700 seconds. Frequency wave-number analysis showed the initial Rayleigh wave arrival from a back azimuth of 300° - 305° and a second arrival about four minutes later from a back azimuth of 315° - 320°. This latter wave was contained in the long window but not in the short window during the coherency estimation. The coherence loss for the short window can be explained by an azimuthal distribution of about $\pm$ 5° and a velocity of $\pm$ 0.1 - 0.2 km/sec. about the mean value.

The rapid fall off in coherence using the longer window suggests a second discrete arrival separated by about 20° from the first and this is in agreement with the frequency-wavenumber analysis. It can be seen that the second arrival has had no effect on the velocity dependent coherence.

The second LASA example is for a Rayleigh wave from an event in Baja California. The propagation path is entirely continental. Inspection of the individual channels in Figure 16 indicates good signal similarity and no apparent interference. However the spatial coherence does show separation in the two orthogonal directions and this can be explained by an azimuthal range of 15° about the mean and a velocity range of $\pm$ 0.2 km/sec.

DISCUSSION

Spatial coherence estimates at array sites help us to understand the propagation of surface waves in a heterogeneous medium.

In addition to the phenomenon of multipathing described by Capon (1970) it would appear that 'pure' surface wave phases do not exhibit a single propagation direction or velocity. The unique wave vector has to be replaced with a distribution, the dimensions of which can be estimated approximately from the coherence. The wavenumber distribution estimated in this way is independent of the array response. However, if the diameter of the array is too small, the functional form of the spatial coherence is left in doubt because all the models suggested in this paper have approximately the same shape for the shorter separation distances and there is sufficient scatter in the estimates so that all the theoretical curves, or combinations of them, tend to fit the measured estimates of the coherence. In this light, it is obvious that the quantitative values given for the wavenumber distribution, reflecting the scattering, must be considered as order-of-magnitude estimates.

The azimuthal variation strongly indicates that at least part of the scattering is a function of the travel path rather than the structure under the array.

The wave scattering phenomenon decreases with increase of period and is very small for periods greater than 40 seconds.

-13-

The fact that the phase velocity at periods of about 20 seconds has a distribution rather than a single value limits the resolution with which this portion of the dispersion curve can be inverted to obtain crustal structure. This distribution is in the range 0.1 - 0.4 km/sec even for 'pure' Rayleigh waves.

REFERENCES

Aki, K., 1957, Space and time spectra of stationary
stochastic waves, with special references to
microtremors: Bull. Earth. Res. Inst., v. 35,
p. 415-457.

Backus, M., Burg, V., Baldwin, D. and Bryan, E., 1964,
Wideband extraction of mantle P waves from ambient
noise: Geophysics, v. 29, No. 5, p. 672-692.

Bungum, H., Rygg, E. and Bruland, L., 1971, Short-
period seismic noise structure at the Norwegian
seismic array: Bull. Seism. Soc. Am., v. 61, No. 2,
p. 357-374.

Capon, J., 1969, Investigation of long-period noise at
the large aperture seismic array: J. Geophys. Res.
v. 74, No. 12, p. 3182-3194.

Capon, J., 1970, Analysis of Rayleigh wave multipath
propagation at LASA: Bull. Seism. Soc. Am., v. 60,
No. 5, p. 1701-1737.

Chernov, L.A., 1960, Wave propagation in a random medium:
New York, Dover Publications, Inc., p. 168.

Glover, P. and Alexander, S.S., 1969, Lateral variations
in crustal structure beneath the Montana LASA:
J. Geophys. Res., v. 74, No. 2, p. 505-531.

Gossard, E.E., 1969, The effect of bandwidth on the
interpretation of the cross-spectra of wave record-
ings from spatially separated sites: J. Geophys.
Res., v. 74, No. 1, p. 325-337.

Gossard, E.E. and Sailors, D.B., 1970, Dispersion band-
width deduced from coherency of wave recordings
from spatially separated sites: J. Geophys. Res.,
v. 75, No. 7, p. 1324.

Mack, H. and Flinn, E.A., 1971, Analysis of the spatial
coherence of short-period acoustic gravity waves
in the atmosphere: Geophys. Journal, v. 26, Nos.
1-4, p. 255-270.

Mack, H., 1972, Evaluation of the LASA, ALPA, NORSAR
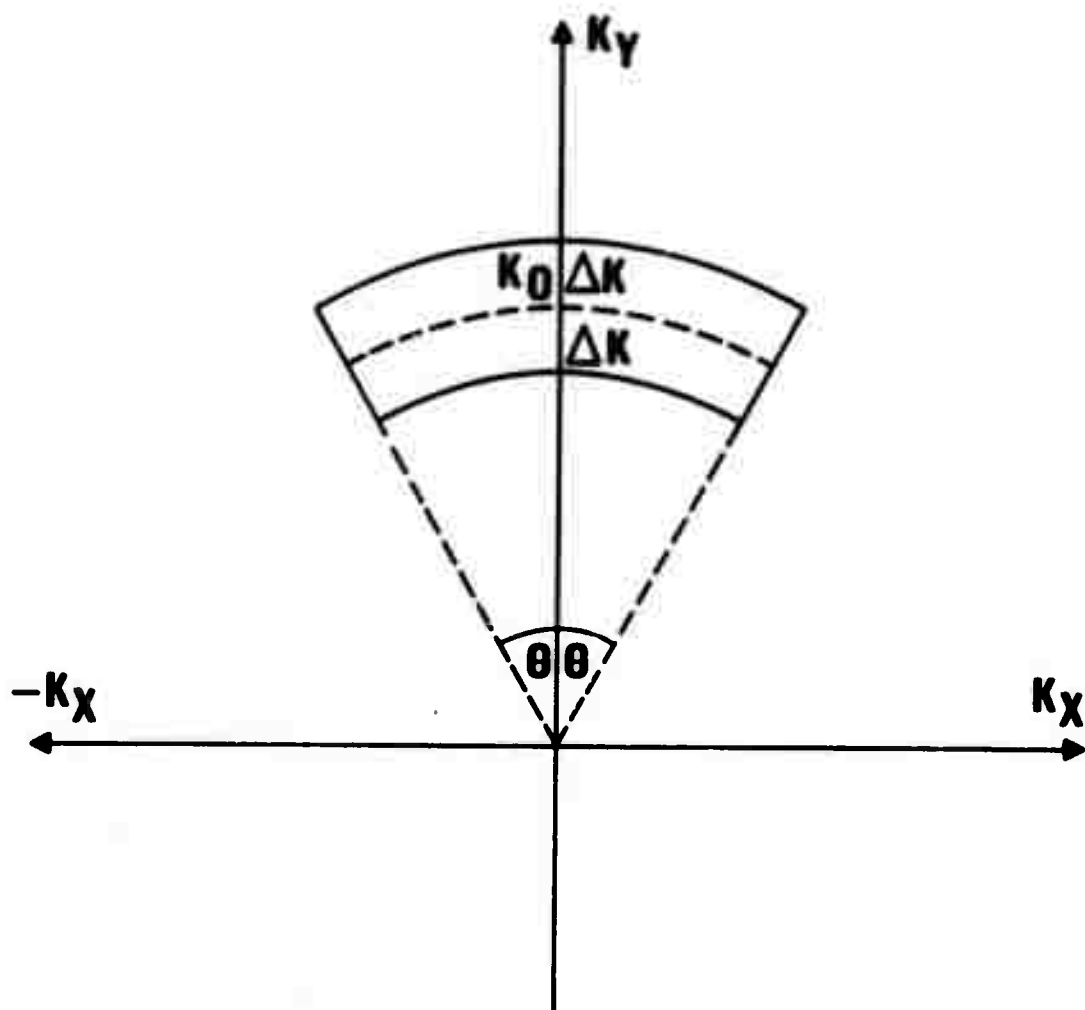long period network: Seismic Array Analysis Center
Report No. 6, Teledyne Geotech, Alexandria,
Virginia.

Figure 1. Wavenumber representation of a wave group propagating with a range of azimuth and velocity.

17
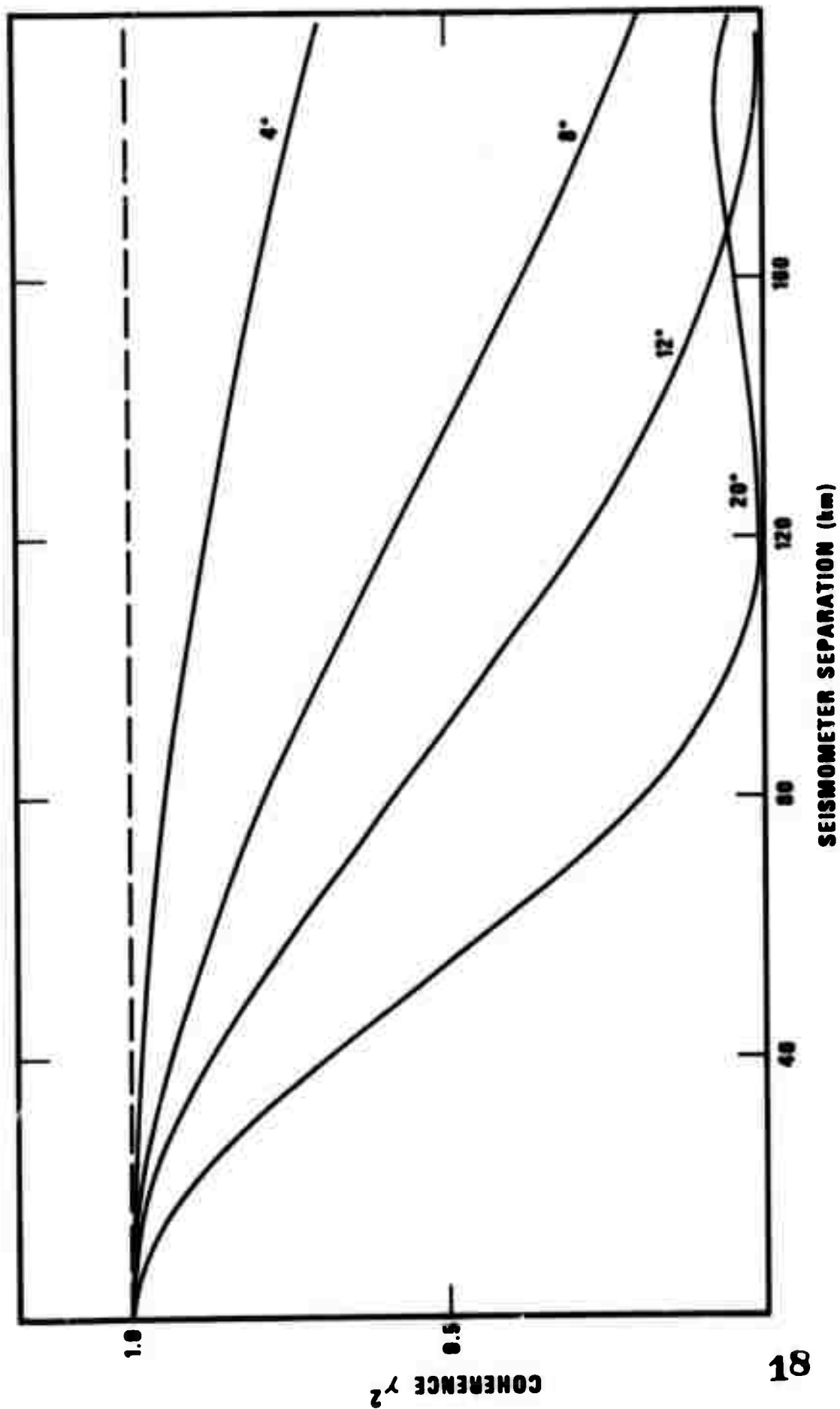
Figure 2. Theoretical coherence versus seismometer separation along the mean wavefront and parametric in range of azimuth of the propagation vector for a period of 21.3 sec (velocity = 4.0 km/sec).

18
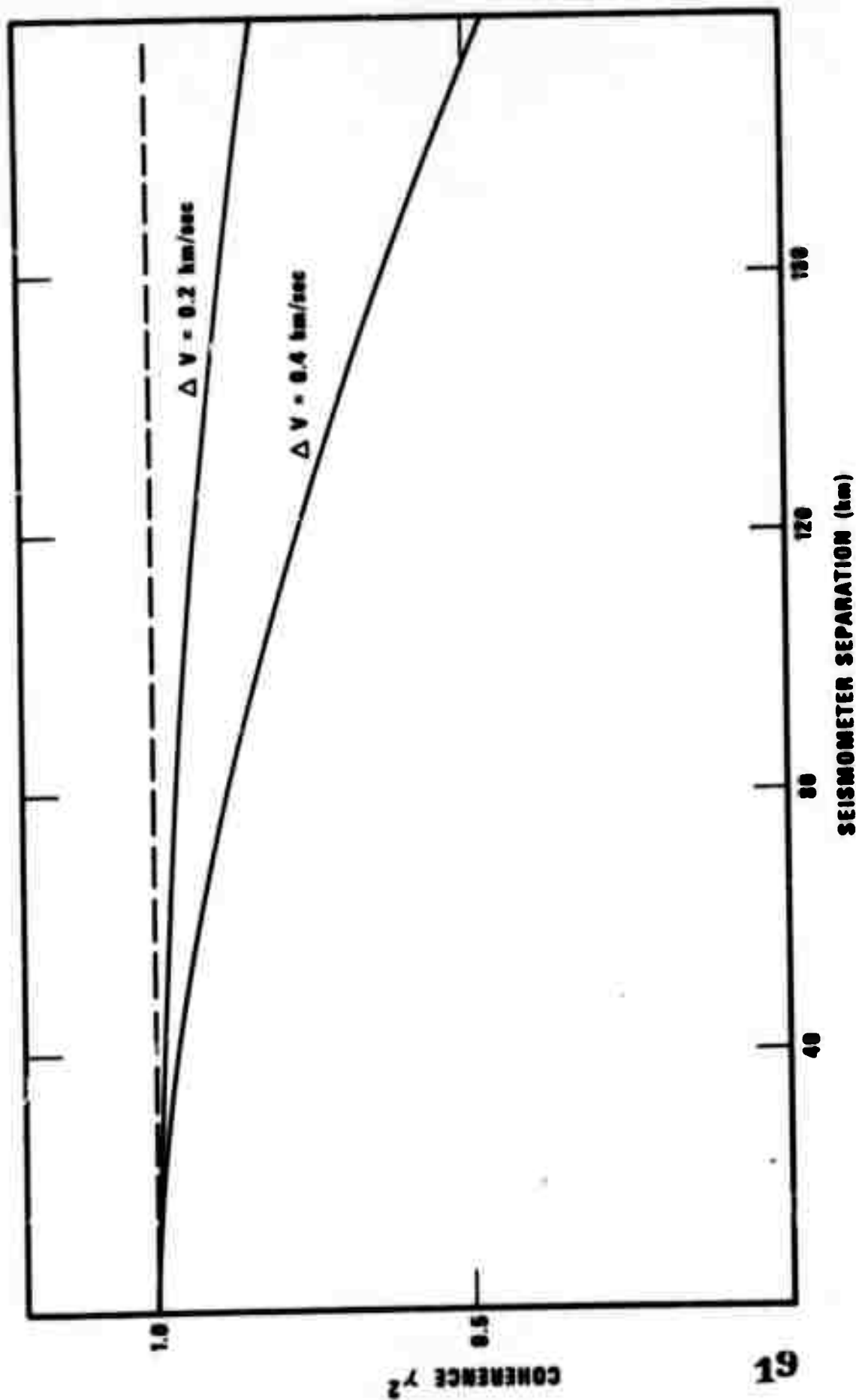
Figure 3. Theoretical coherence versus seismometer separation in the mean direction of propagation and parametric in the range of phase velocity for a period of 21.3 sec.

19
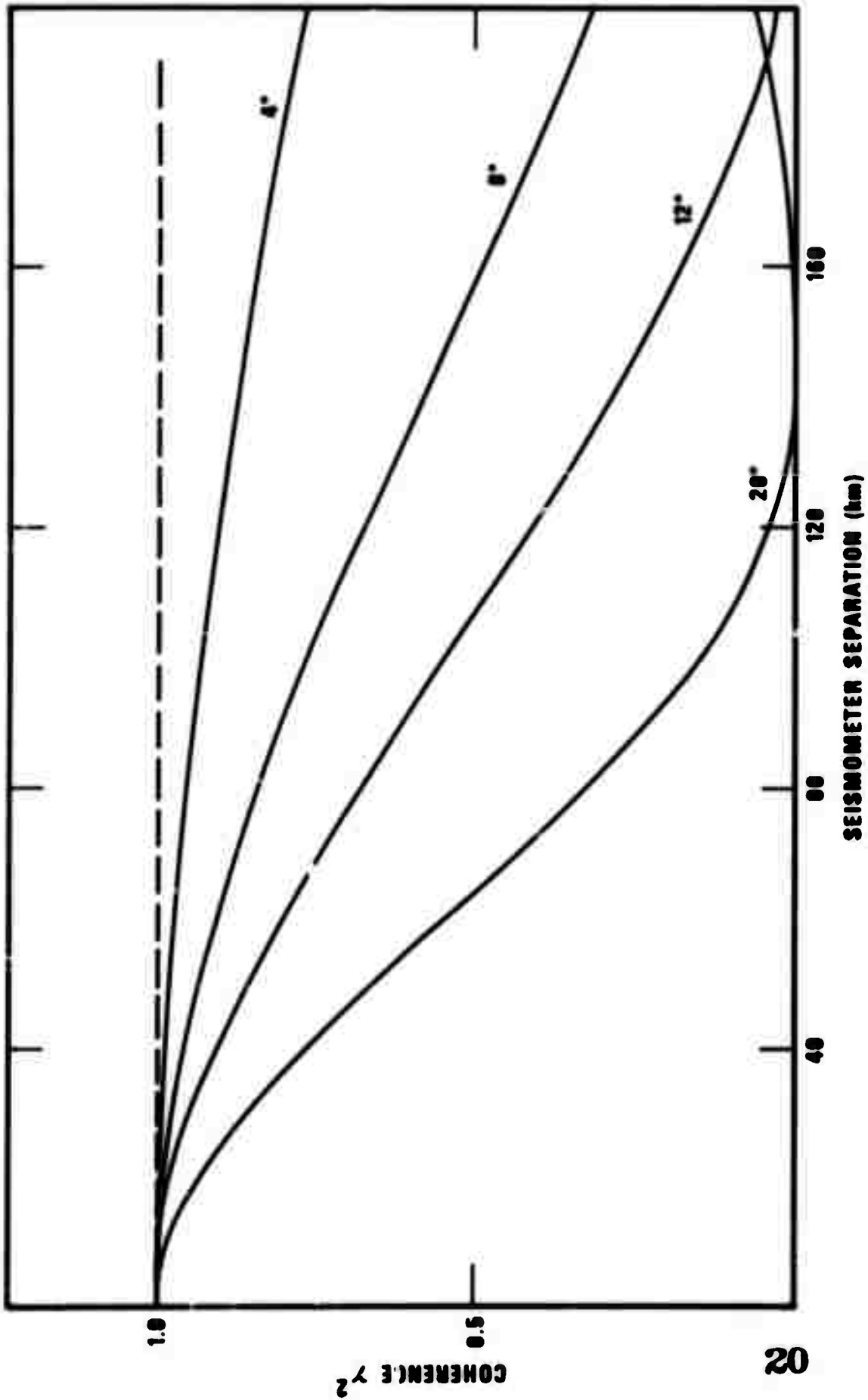
Figure 4. Theoretical coherence versus seismometer separation along the mean wavefront and parametric in range of azimuth of the propagation vector for a period of 25.6 sec (velocity = 4.0 km/sec).
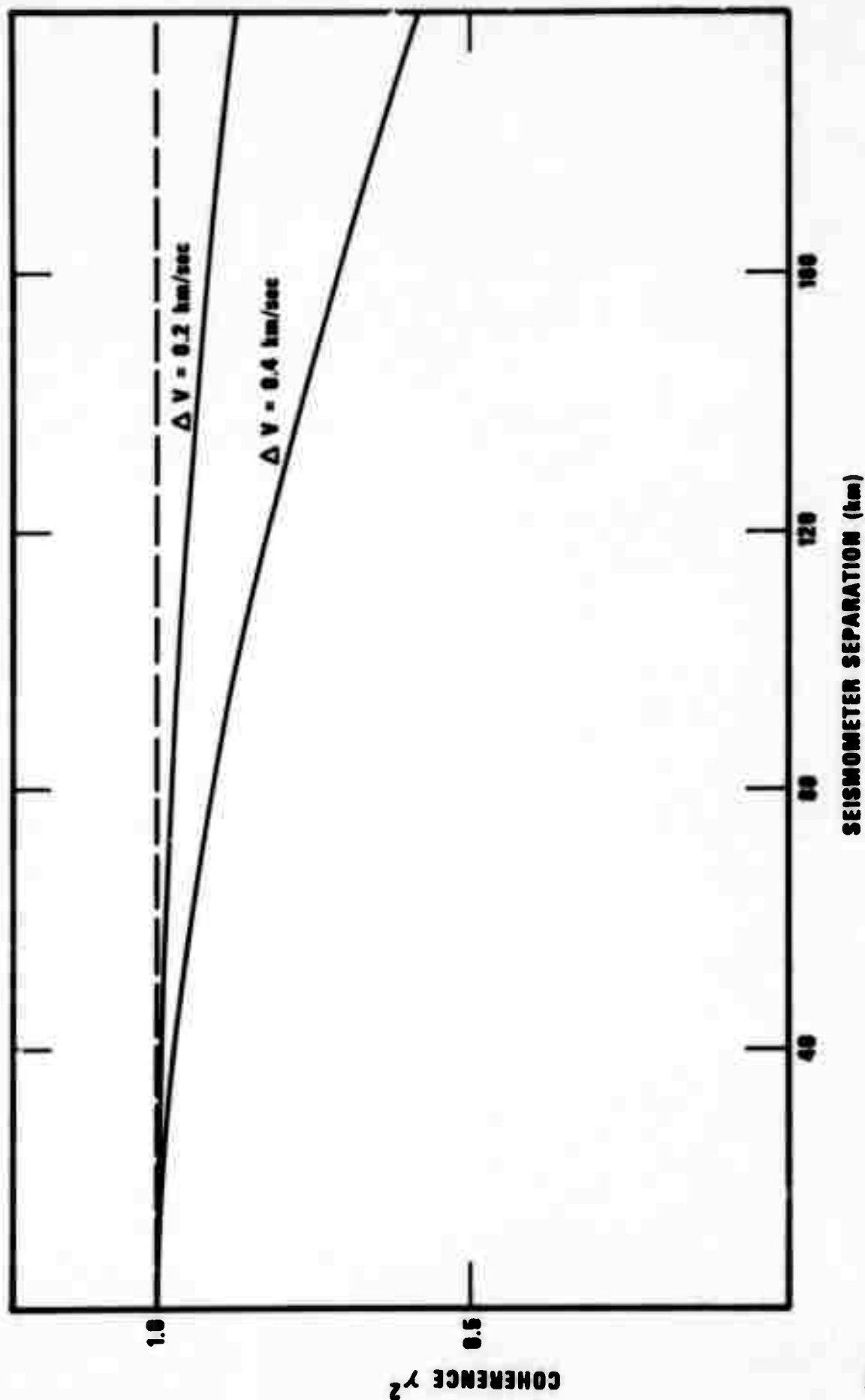
Figure 5. Theoretical coherence versus seismometer separation in the mean direction of propagation and parametric in the range of phase velocity for a period of 25.6 sec.

21
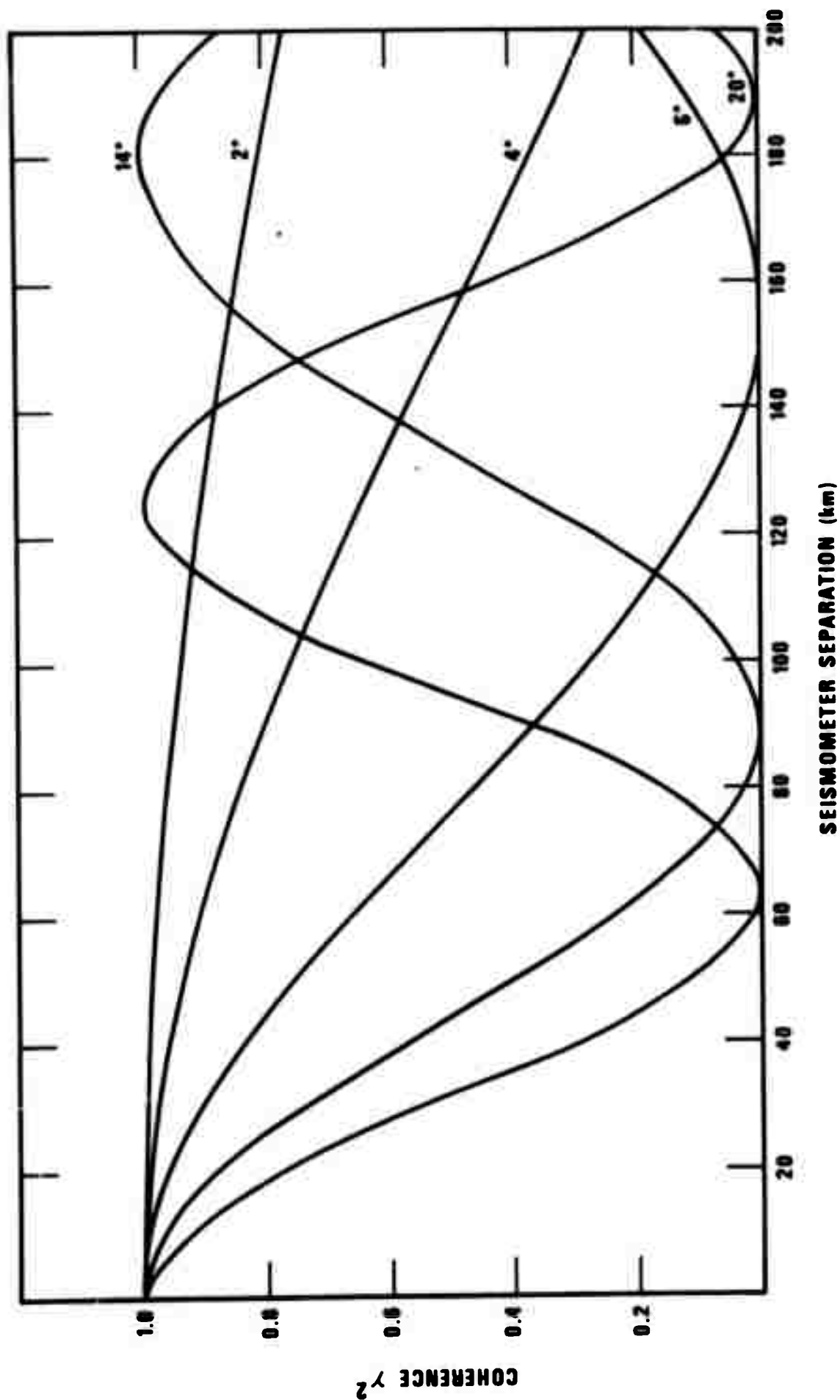
Figure 6. Theoretical coherence versus seismometer separation along mean wavefront and parametric in azimuthal separation between two discrete waves for a period of 21.5 seconds.

COHERENCE γ²

SEISMOMETER SEPARATION (km)

22
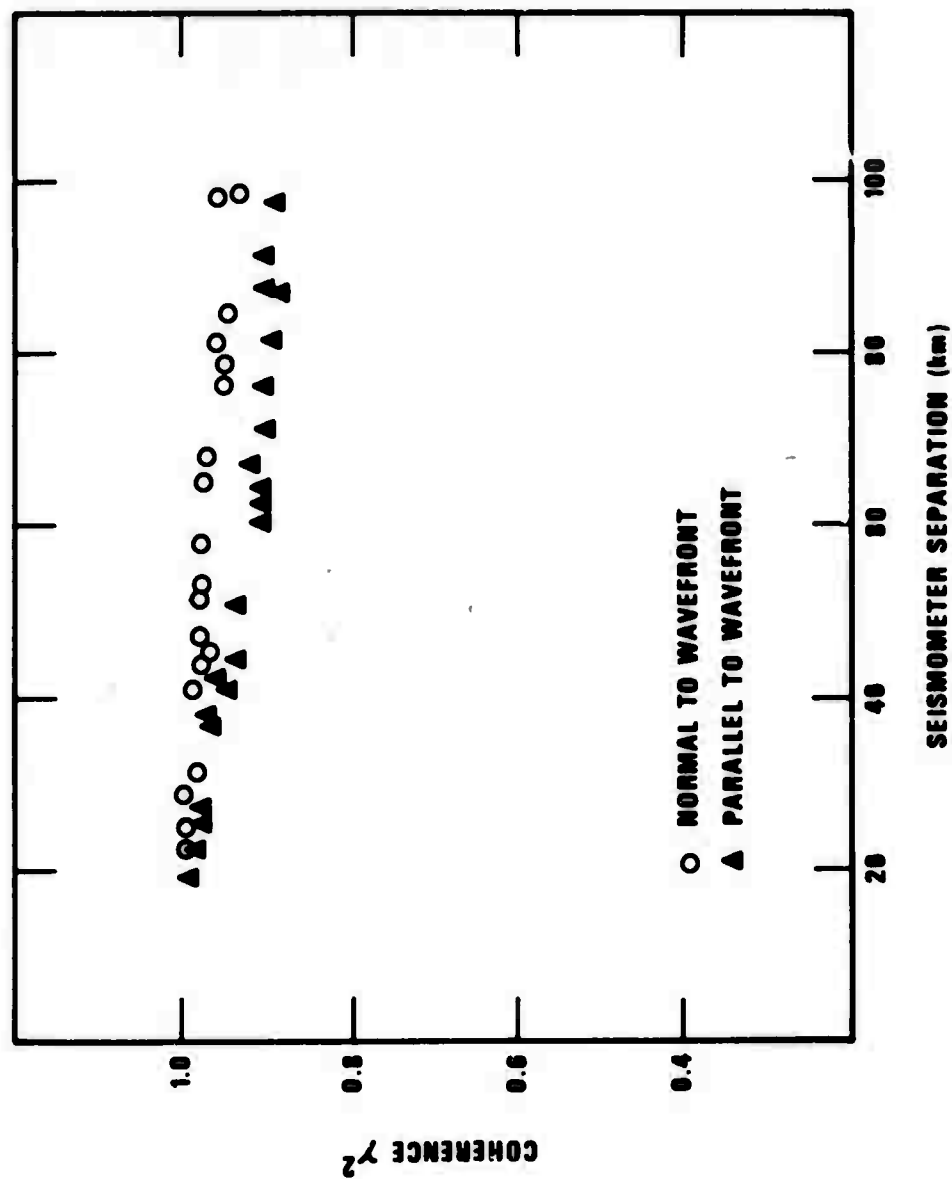
Figure 7. Coherency at a period of 21.3 sec versus seismometer
separation for the Rayleigh wave shown in Figure 8.
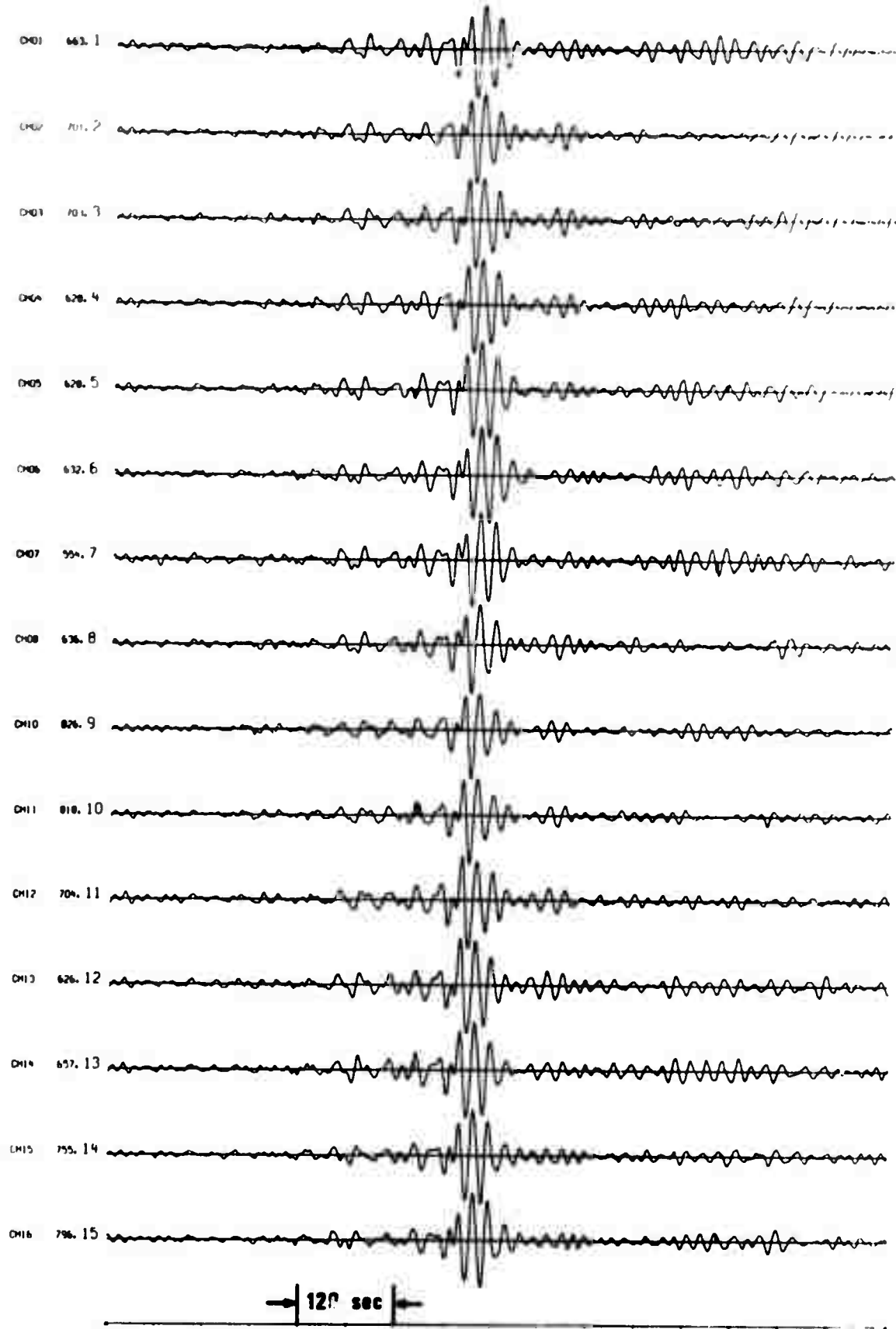
Figure 8. Individual channel recordings at NORSAR of the Rayleigh wave from North Sinkiang. Date, 1 November 1971; origin time, 05:29:57.2, Δ = 45°.

24
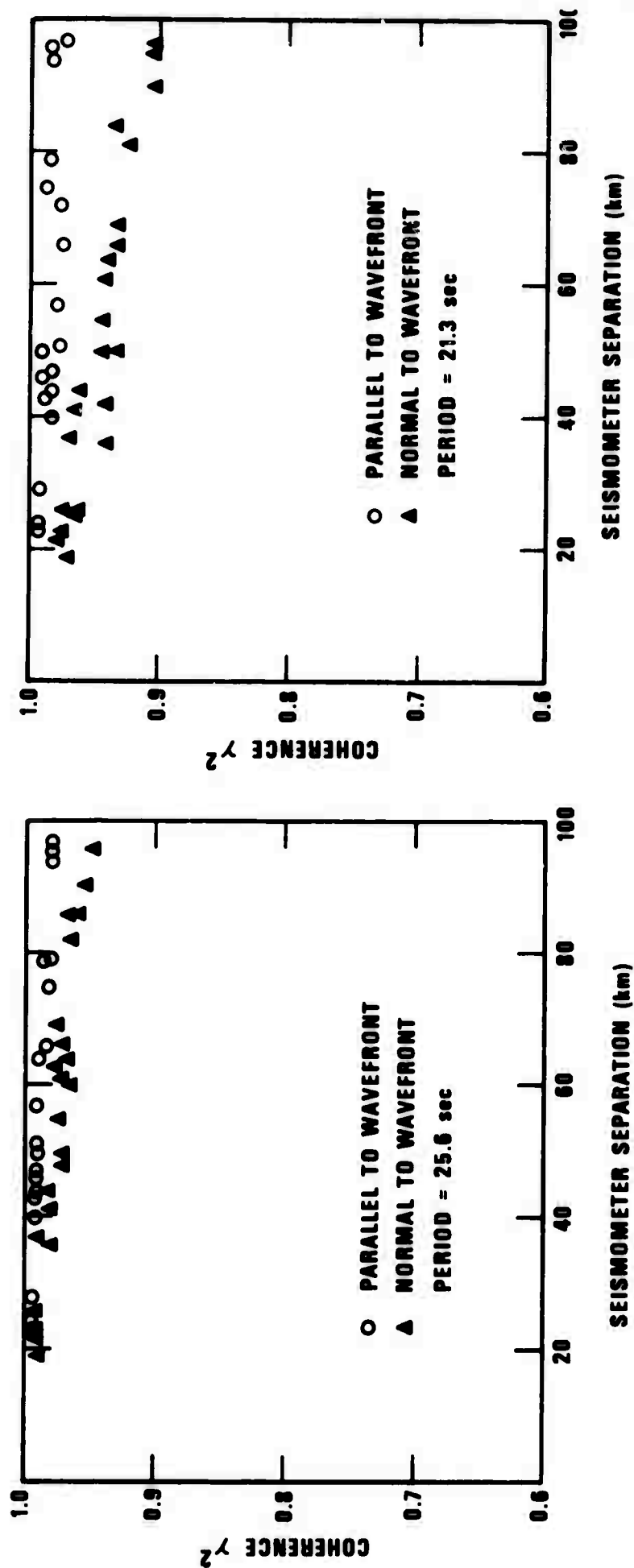
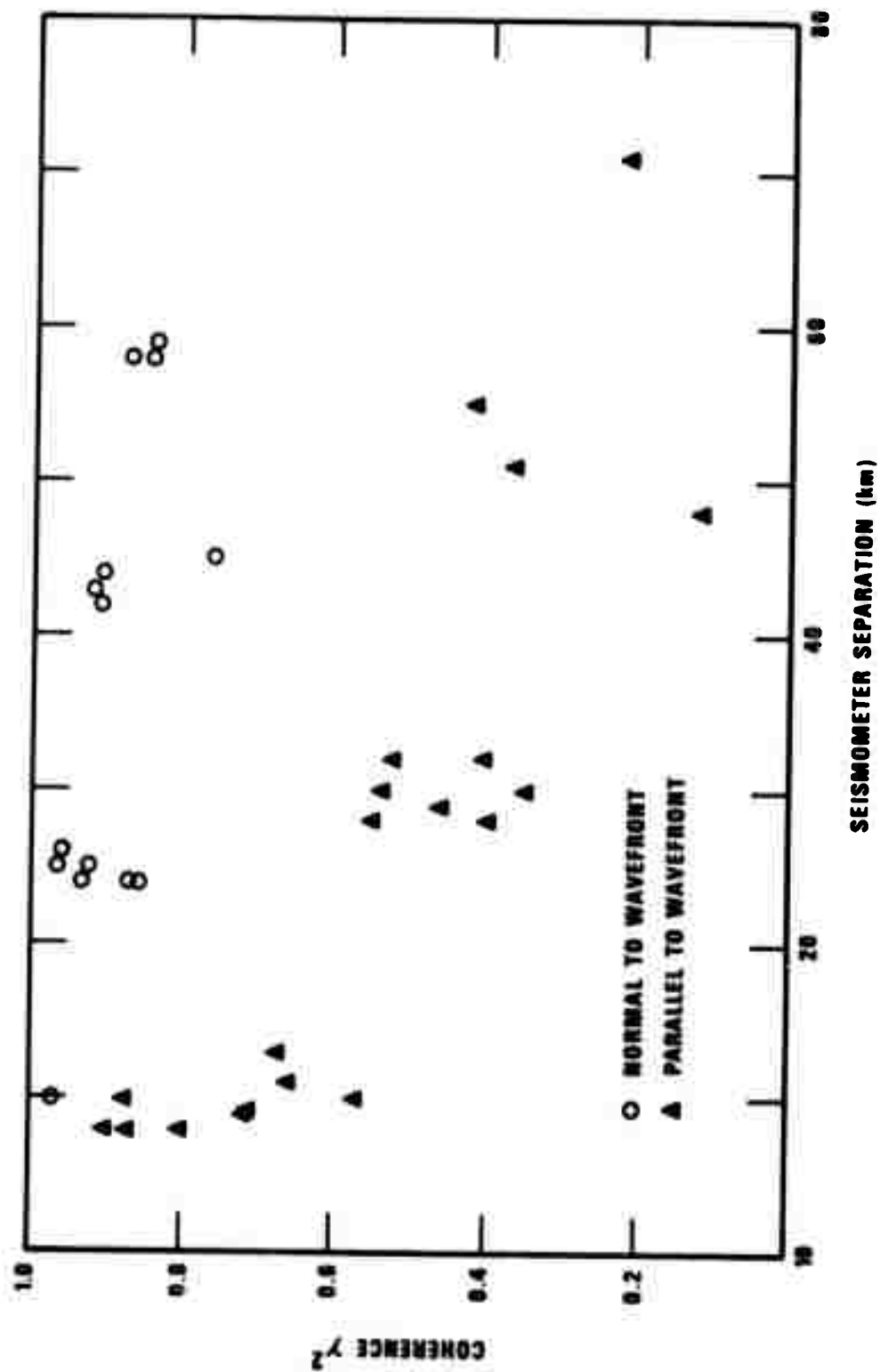Figure 9. Coherency versus seismometer separation for the Love wave from North Sinkiang recorded at NORSAR.

25
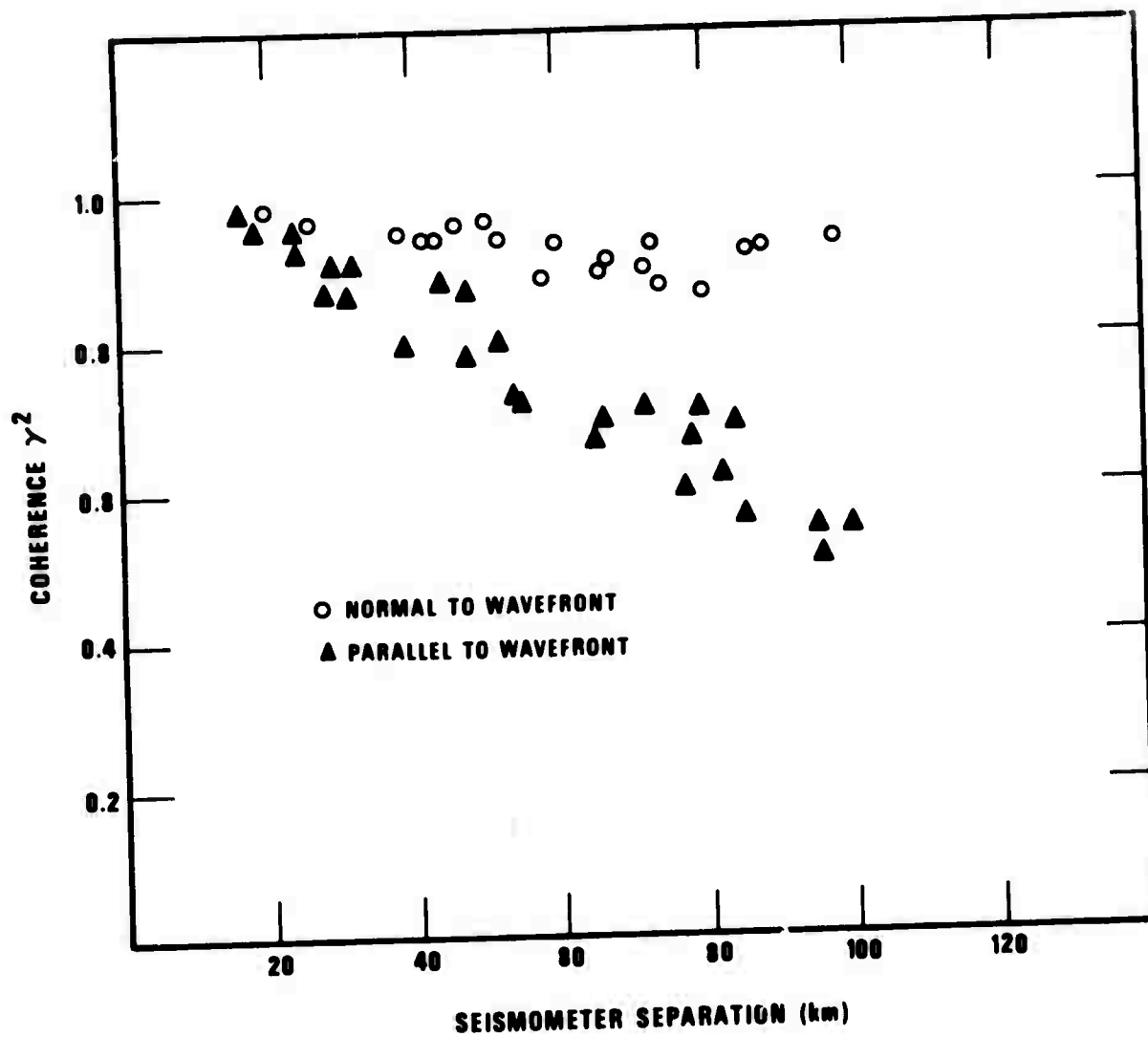
Figure 10. Coherency at a period of 21.3 sec versus seismometers separation for the Rayleigh waves shown in Figure 11.
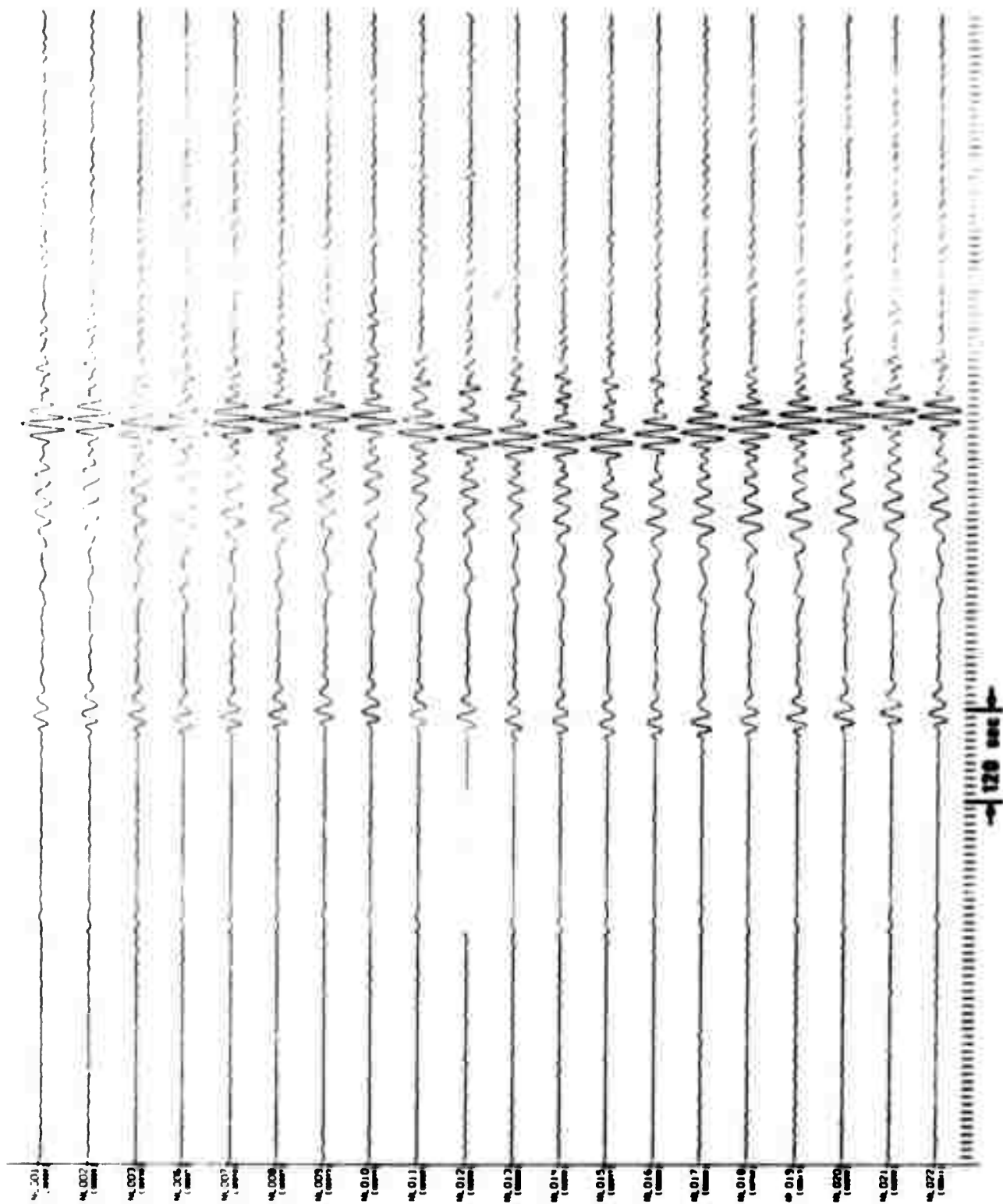
Figure 11. Rayleigh waves recorded at NORSAR from an earthquake in Turkey. Date, 6 May 1971; origin time, 04:30:04, Δ = 25°.
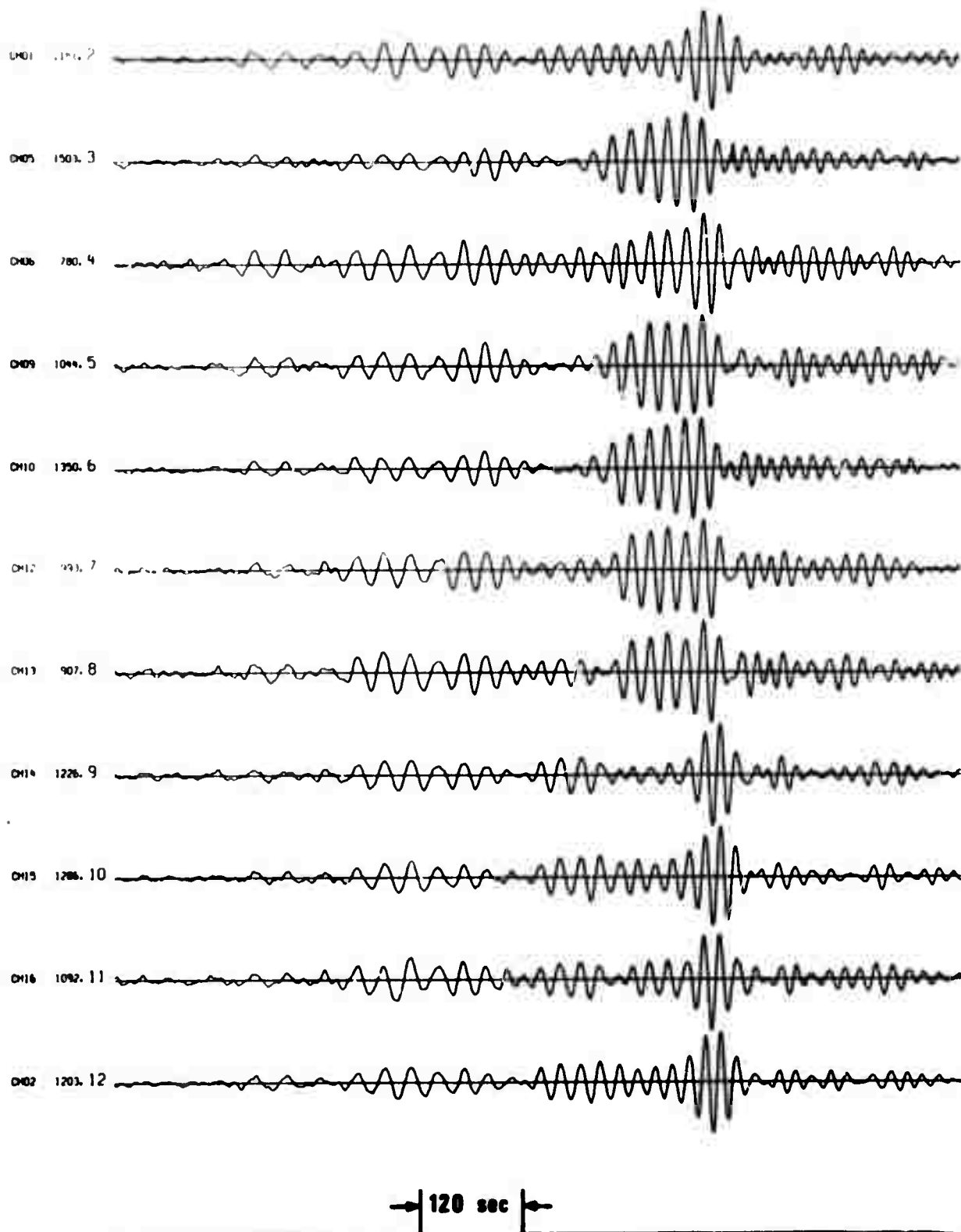
Figure 12. Rayleigh waves recorded at ALPA from the event in North Sinkiang. Date, 1 November 1971; origin time, 05:29:57.2, Δ = 62°.

Figure 13. Coherency at a period of 21.3 sec versus seismometer separation at ALPA for the Rayleigh wave shown in Figure 12.
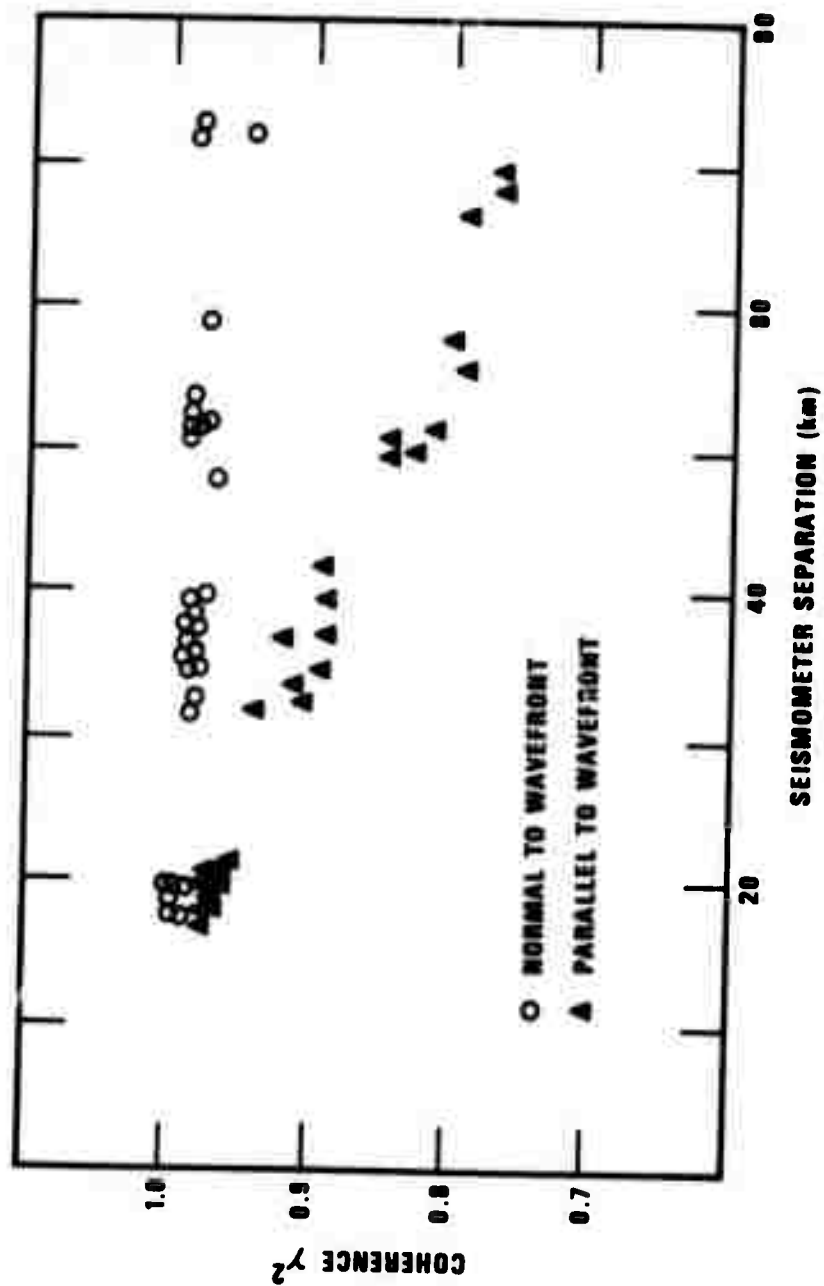
Figure 14. Coherency at a period of 21.3 sec versus seismometer separation at ALPA for Rayleigh waves from CANNIKIN, $\Delta = 21°$.
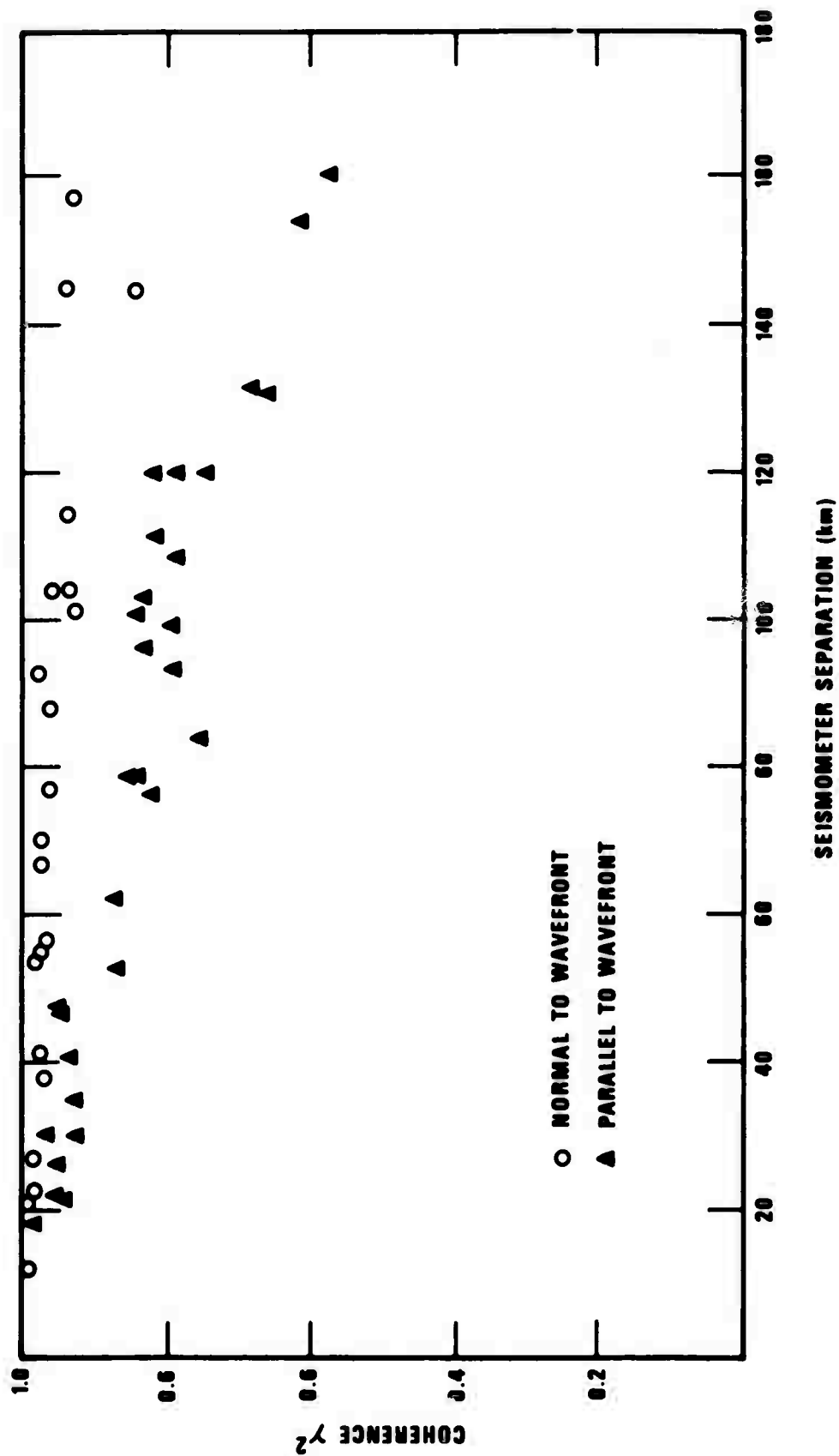
30

Figure 15a. Spatial coherency estimates on the first 400 sec of a Rayleigh wave from an earthquake in the Andreanoff Islands. Date, 30 March 1971; origin time, 11:30:38.9, Δ = 43°.
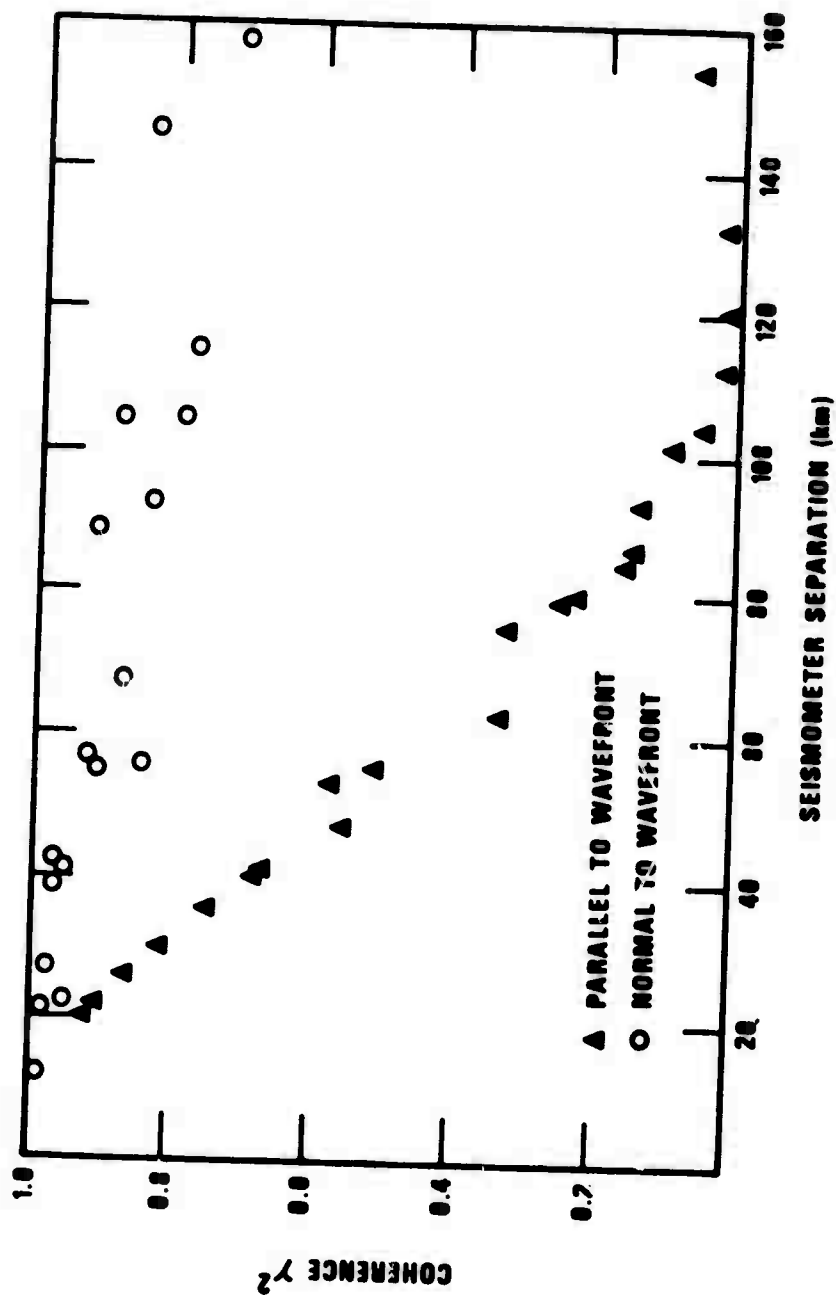
31

Figure 15b. Spatial coherence using the first 700 sec of the Rayleigh wave. The rapid drop in coherence along the wavefront indicates the presence of a multipathed arrival.
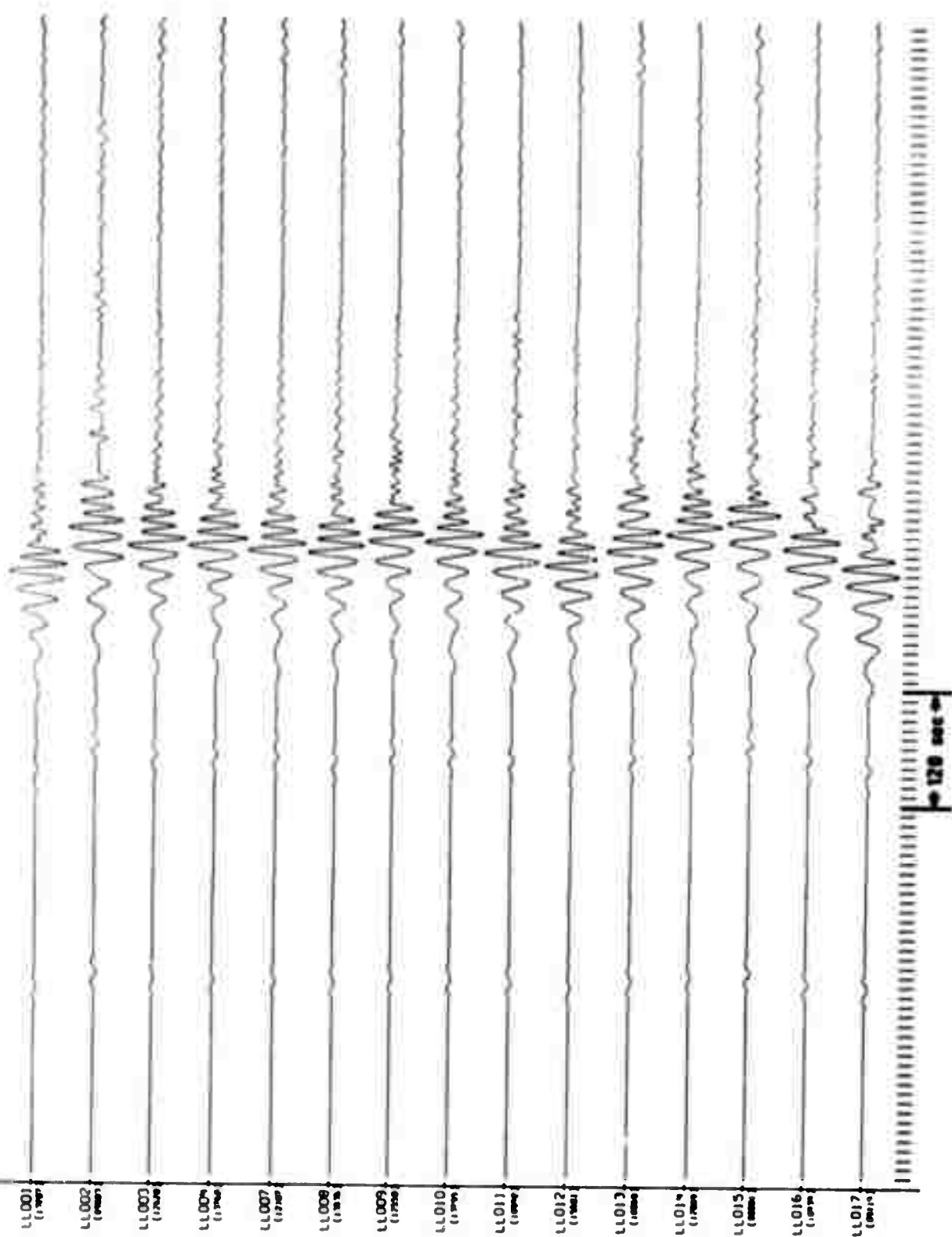
Figure 16. Rayleigh waves recorded at LASA from an earthquake in Baja California. Date, 14 April 1971; origin time, 11:43:06. Δ = 21°.
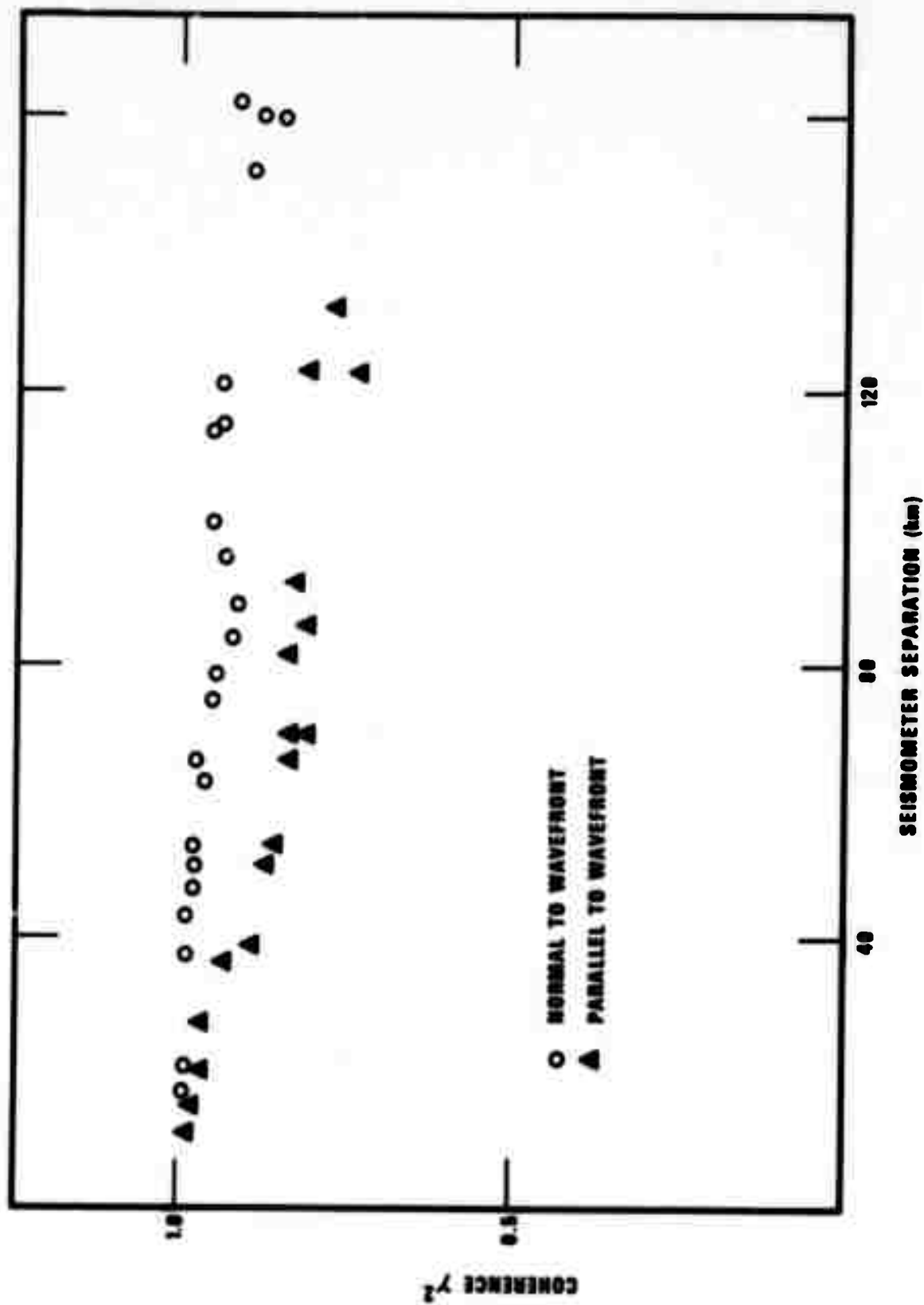
33

Figure 17. Coherency at 21.3 sec period versus seismometer separation for the Rayleigh waves shown in Figure 16.

34